

# Excitation and damping of collective modes of a Bose-Einstein condensate in a one-dimensional lattice

O. Morsch<sup>1</sup>, J.H. Müller<sup>1</sup>, D. Ciampini<sup>1</sup>, M. Cristiani<sup>1</sup>, P.B. Blakie<sup>2</sup>, C.J. Williams<sup>2</sup>, P.S. Julienne<sup>2</sup>, and E. Arimondo<sup>1</sup>

<sup>1</sup> INFN, Dipartimento di Fisica E. Fermi, Università di Pisa, Via Buonarroti 2, I-56127 Pisa, Italy

<sup>2</sup> National Institute of Standards and Technology, Gaithersburg, Maryland 20899-8423.

(March 22, 2002)

The mode structure of a Bose-Einstein condensate non-adiabatically loaded into a one-dimensional optical lattice is studied by analyzing the visibility of the interference pattern as well as the radial profile of the condensate after a time-of-flight. A simple model is proposed that predicts the short-time decrease of the visibility as a function of the condensate parameters. In the radial direction, heavily damped oscillations are observed, as well as an increase in the condensate temperature. These findings are interpreted as a rethermalization due to dissipation of the initial condensate excitations into high-lying modes.

PACS number(s): 03.75.Fi, 32.80.Pj

Studying collective modes in a Bose-Einstein condensate (BEC) is an efficient method for obtaining information about the dynamics of this quantum system [1,2]. So far, both experimental and theoretical results have been obtained for low-lying modes of a condensate in a magnetic trap, including breathing modes [3], surface modes [4] and the scissors mode [5]. Typically, in these experiments the collective modes were excited by a sudden change in the trap frequency or geometry, and the frequency and damping rate [6] of the subsequent oscillations were measured either in situ or after a time-of-flight.

In this paper we present experimental results and some preliminary theoretical considerations on the mode structure of a Bose-Einstein condensate inside a one-dimensional periodic potential. In experiments to date, BECs have been loaded into optical lattices mainly in the adiabatic regime in order to study, e.g., number squeezing [7] and the Mott-insulator transition [8]. In this context, 'adiabatic' refers to the modes of the entire condensate rather than the single-well oscillation frequency. Therefore, the condition for adiabaticity is  $\tau_{\text{ramp}} \gg (\hbar/\mu)^{1/2}$ , where  $\tau_{\text{ramp}}$  is the time over which the periodic potential is ramped up, and  $\mu$  is the chemical potential of the condensate [9]. By violating this condition (but still satisfying  $\tau_{\text{ramp}} \gg 2\pi/\omega_{\text{lat}}$ , with  $\omega_{\text{lat}}$  the single-well harmonic oscillator frequency), collective modes are excited in the condensate.

Our experimental setup is described in detail elsewhere [10,11]. After creating BECs of  $N_0 = 1.5(5) \times 10^4$   $^{87}\text{Rb}$  atoms [12] in a triaxial time-orbiting potential trap, we adiabatically lower the trap frequency  $\omega_{\text{trap}}$  to the desired value and then superimpose onto the magnetic

trap an optical lattice along the vertical trap axis (for which the trap frequency  $\omega_{\text{long}} = \omega_{\text{trap}}$ ) created by two linearly polarized Gaussian laser beams intersecting at a half-angle  $\theta = 18$  degrees and detuned by 30 GHz above the rubidium resonance line. The periodic potential  $V(z) = V_0 \sin^2(kz)$  thus created has a lattice spacing  $d = 1.2 \mu\text{m}$ , and the depth  $V_0$  of the potential (measured in lattice recoil energies  $E_{\text{rec}} = \hbar^2 k^2 / 2m$ ) can be varied between 0 and  $20 E_{\text{rec}}$  by adjusting the laser intensity using acousto-optic modulators. The number of lattice sites occupied by the condensate lay between 10 and 15, depending on the trap frequency.

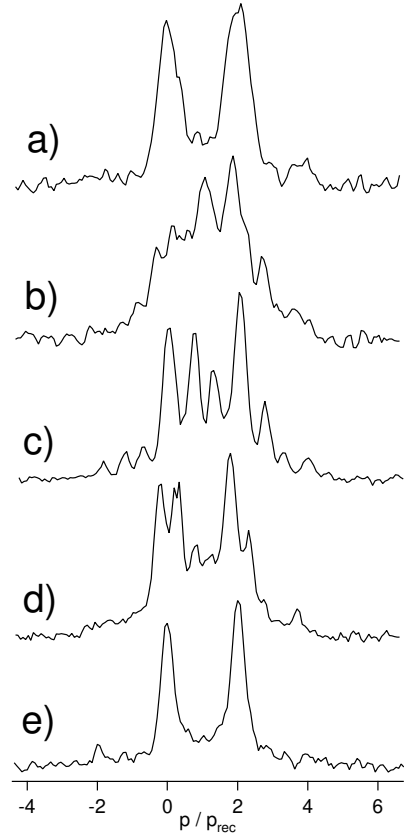


FIG. 1. Evolution of the interference pattern (integrated perpendicular to the lattice direction) of a condensate released from an optical lattice after non-adiabatic loading. The distinct two-peaked structure visible immediately after loading (a) is washed out within the first few milliseconds (b), after which the interference pattern takes on a complex structure ((c) and (d)). For long holding times, the initial two-peaked structure reappears (e). In this experiment,  $\bar{\omega}_{\text{trap}} = 26.7 \text{ Hz}$ ,  $\tau_{\text{ramp}} = 5 \text{ ms}$ , and  $V_0 = 15 E_{\text{rec}}$ . From (a) to (e),  $t_{\text{hold}} = 1; 22; 50; 100$  and  $300 \text{ ms}$ , respectively.

In a typical experiment, the optical lattice was ramped up in  $\tau_{\text{ramp}} = 1 \text{ ms}$ , after which the potential was kept at its maximum value  $V_0$  for a holding time  $t_{\text{hold}}$ . At the end of the holding time, the lattice was accelerated in  $1 \text{ ms}$  to one (lattice) recoil velocity by chirping the frequency difference between the lattice beams. Immediately after that, both the lattice and the magnetic trap were switched off. After a time-of-flight of  $20 \text{--} 22 \text{ ms}$ , the expanded condensate was imaged using a resonant probe flash. Figure 1 shows typical integrated absorption images obtained in this manner for different holding times. For short times, a clean double-peak structure is visible, as expected from the interference between the condensates expanding from the individual lattice wells (with a phase difference between them due to the final acceleration). During the first few milliseconds, this pattern evolves into a more complicated structure featuring several additional peaks, and finally washes out completely, resulting in a single Gaussian-shaped lump. In an intermediate regime ( $t_{\text{hold}} = 20 \text{--} 100 \text{ ms}$ ), the interference pattern again becomes complex, with multiple peaks. For longer waiting times, the two-peaked structure reappears.

We analyzed our experimental data in two different ways. In the lattice direction, we characterized the interference pattern (integrated perpendicular to the lattice direction) through a visibility calculated as

$$V = \frac{h_{\text{peak}} - h_{\text{middle}}}{h_{\text{peak}} + h_{\text{middle}}}; \quad (1)$$

where  $h_{\text{peak}}$  is the mean value of the absorption image at the position of the two peaks, and  $h_{\text{middle}}$  is the value of the absorption image midway between the two peaks (averaged over a range of  $l=5$  of the peak separation). In the direction perpendicular to the optical lattice, we fitted a bimodal Gaussian function to the (longitudinally) integrated absorption profile and extracted from this  $t$  the condensate fraction and the width  $\sigma_{\text{perp}}$  of the condensate part.

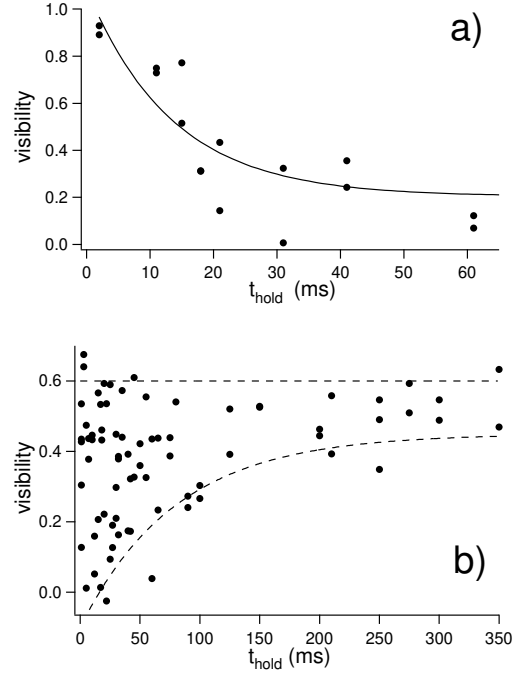


FIG. 2. Examples of the short-term (a) and long-term behaviour (b) of the visibility for a condensate in an optical lattice after non-adiabatic loading. In (a), the initial loss of visibility is evident (solid line: exponential fit with time constant  $13 \text{ ms}$ ). The trap frequency  $\bar{\omega}_{\text{trap}} = 19.8 \text{ Hz}$ , and  $V_0 = E_{\text{rec}} = 15$  with  $\tau_{\text{ramp}} = 1 \text{ ms}$ . In (b), after strong initial fluctuations the visibility approaches a stable value close to the initial visibility. In this experiment,  $\bar{\omega}_{\text{trap}} = 26.7 \text{ Hz}$ ,  $V_0 = E_{\text{rec}} = 15$  and  $\tau_{\text{ramp}} = 5 \text{ ms}$ . The dashed lines are an envelope to the data points with a constant upper part and an exponential lower part with a time constant of  $\approx 80 \text{ ms}$ .

Figure 2 shows examples of the short-term and long-term behaviour of  $V$ . Initially,  $V$  rapidly decreases from a value of  $0.6 \text{--} 0.9$  to roughly 0 within  $5 \text{--} 20 \text{ ms}$ , depending on the trap frequency  $\bar{\omega}_{\text{trap}}$ . Subsequently,  $V$  typically rises again and begins to fluctuate in an apparently random manner for a few tens of milliseconds. Finally, these fluctuations die out and  $V$  stabilizes at a value close to the initial visibility.

The corresponding behaviour of the condensate width  $\sigma_{\text{perp}}$  and temperature (calculated from the condensate fraction) is shown in Fig. 3. One clearly sees radial oscillations of  $\sigma_{\text{perp}}$  at a frequency  $\omega_{\text{osc}} = 2 \sigma_{\text{perp}}$ , where  $\sigma_{\text{perp}} = \frac{\bar{\omega}_{\text{trap}}}{2}$  is the trap frequency perpendicular to the lattice direction. These oscillations are heavily damped with a quality factor  $Q = 2 \omega_{\text{osc}} \tau_{\text{damp}} = 10 \text{--} 30$ . Simultaneously, the condensate temperature expressed as  $T = T_c$  (where  $T_c$  is the critical temperature for the BEC transition) increases and approaches a new steady-state value on a time scale comparable to  $1/\tau_{\text{damp}}$ .

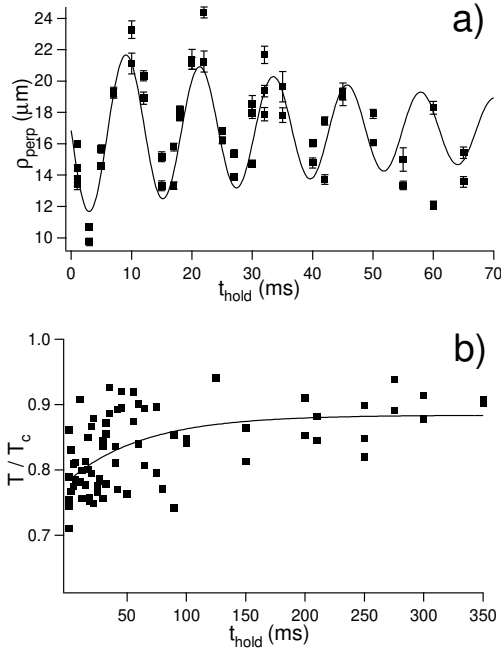


FIG. 3. Time evolution of the width (a) and the temperature (b) of the condensate in the optical lattice (same trap and lattice parameters as in Fig. 2 (b)). The solid lines are fits to the data using an exponentially damped sinusoidal oscillation in (a) and a simple exponential function in (b). In both cases, the time constants of the exponential part are 70 ms. Note the different time scales in the two graphs.

The short-term decrease in  $T/T_c$  can be explained using a simple model. We take the Bose-Einstein condensate wavefunction to evolve according to the Gross-Pitaevskii equation

$$i\hbar \frac{\partial \psi}{\partial t} = -\frac{\hbar^2}{2m} \nabla^2 \psi + \frac{1}{2} m \sum_j \omega_j^2 x_j^2 \psi + V_0(t) \sin^2 \frac{z}{d} \psi + U \psi^2 \psi; \quad (2)$$

where  $x_j = fx; y; zg$  are the spatial coordinates along which the respective trap frequencies are  $\omega_j$  ( $= 2\pi f_j$ ),  $U = 4\pi\hbar^2 a/m$  is the collisional interaction strength with  $a = 5.4 \text{ nm}$  the s-wave scattering length.

The rate at which the lattice is raised is slow enough that band excitations can be ignored and the condensate density will be reshaped to lie at the potential minima of each lattice site. Because we are interested in the phase properties of the entire condensate, it is convenient to consider a continuous Wannier [14] or envelope representation [15] of the wavefunction, where we define the envelope  $f(x; t)$  to represent the slowly varying amplitude of the Gross-Pitaevskii wavefunction  $\psi(x; t)$ , in which the rapid density variation along the lattice is smoothed out (also see [13]). The evolution equation for  $f$  is of a similar form to Eq. (2) except that the lattice potential no longer appears explicitly; the diffusion along  $z$  is

generated by the Bloch dispersion relation reflecting the modified tunneling properties in this direction; and the mean-field term is renormalized as  $U \psi^2 \psi \rightarrow (1 + c)U f^2 f$  resulting from the compressed condensate density in the lattice. In the tight binding limit the Wannier states are localized and can be approximated by the harmonic oscillator orbital  $w(z) = \exp(-z^2/2a_{ho}^2) = \frac{1}{\sqrt{a_{ho}}}$ , where  $a_{ho} = \hbar/m\omega_{lat}$  is the oscillator length and  $\omega_{lat} = \sqrt{2V_0/m d^2}$  is the oscillation frequency about the lattice minima. In this limit the renormalized mean-field term is given by  $c = (d \int w(z)^4 dz - 1) = (4mV_0 d^2 = 2\hbar^2 - 1)$  [17], with the validity condition  $a_{ho} \ll d$ .

To develop an approximate expression for the short time dephasing behavior of the condensate we assume that during the lattice loading and subsequent time over which the dephasing occurs density transport in the condensate is negligible, i.e. the evolution occurs in the phase of the wavefunction. In the lattice direction the tunneling frequency determines the time scale over which this assumption will be valid, which is typically of order 100 ms in experiments where dephasing is observed. We also find that for a given trap frequency, there always exists a minimum lattice depth below which no dephasing occurs.

Expressing the envelope function in terms of amplitude and phase as  $f = \sqrt{\rho} \exp(iS)$ , and neglecting the effects of spatial diffusion, the envelope equation of motion reduces to

$$\hbar \frac{\partial S}{\partial t} = \frac{1}{2} m \sum_j \omega_j^2 x_j^2 + U(1 + c)\rho \sqrt{\rho}; \quad (3)$$

Ignoring density transport  $\rho \sqrt{\rho}$  can be approximated by the Thomas-Fermi density profile for the condensate in the initial harmonic trap, which is of the form  $\rho_{TF}(x) \sqrt{\rho} = n_0 [1 - \sum_j (x_j/R_j)^2]$ , where  $n_0$  is the peak density and  $R_j = \sqrt{\hbar^2/m\omega_j^2}$  are the Thomas-Fermi radii [16]. With this substitution the phase evolves as

$$S(x; t) = \frac{cn_0 U t}{\hbar} - \frac{z^2}{R_z^2} + S_0(t); \quad (4)$$

where  $S_0(t)$  is a spatially constant phase. This result shows that the condensate develops a quadratic phase profile along the lattice arising from the imbalance of mean-field and harmonic trap potential energy in the lattice, and is equivalent to a spread in the quasimomentum distribution of the system.

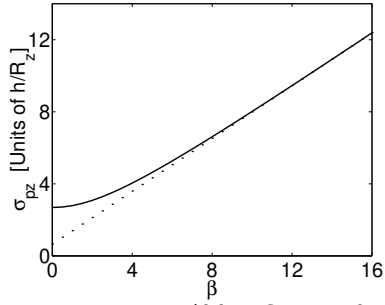


FIG. 4. Momentum width of a condensate with a Thomas-Fermi density distribution and a quadratic phase profile. Numerical calculation (solid), linear fit (dotted).

For a large lattice the quasi momentum distribution of the condensate and the momentum distribution of the envelope function are identical if the momentum distribution lies entirely within the first Brillouin zone. We have calculated the momentum width of the z-component of momentum  $p_z$  for a wavefunction of the form  $\psi(\mathbf{x}; t) = \psi_{TF}(\mathbf{x}) \exp[i(z=R_z)^2]$ , where  $\psi_{TF}$  is the total phase difference between the center and the outside of edge of the condensate. The results (shown in Fig. 4) indicate that for  $\beta > 2$ , the momentum width linearly increases with  $\beta$  and is well approximated by  $\sigma_{pz}(\beta) \approx 0.73 \hbar R_z \beta$ . Identifying  $\beta$  with the coefficient of the quadratic spatial phase term in Eq. (4), we see that the width of the momentum distribution increases linearly with time.

The condensate will initially appear dephased when the quasi momentum width significantly fills the first Brillouin zone, which has a half width of  $\hbar=2d$ . The exact portion of the Brillouin zone which must be filled depends on the observable used to determine the dephasing and may be taken as a fitting parameter. Here we take  $\sigma_{pz} = \hbar/4d$  as the requirement for dephasing, which can be inverted using expression (4) to yield the dephasing time

$$\tau_{\text{deph}} = \frac{R_z \hbar}{2.9 \epsilon \hbar n_0 U} : \quad (5)$$

Figure 5 shows  $\tau_{\text{deph}}$  as a function of  $\nu_{\text{long}}$  (which determines  $R_z$  and  $n_0$ ) together with experimentally measured dephasing times. Equally good agreement with experiment is found when calculating  $\tau_{\text{deph}}$  for the parameters of [7].

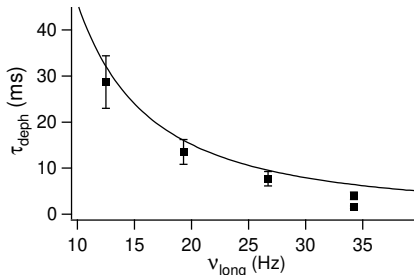


FIG. 5. Experimental dephasing times as a function of the trap frequency  $\nu_{\text{long}}$  in the lattice direction. The solid line is the theoretical prediction for  $\tau_{\text{deph}}$  (see text).

For the intermediate and long-term behaviour of the visibility, the phase-winding model predicts partial and complete revivals of the relative phases, leading to a complicated time-evolution of  $V$ . Experimentally, we see a rather erratic behaviour of  $V$  for intermediate times, with the visibility fluctuating between 0.02 and 0.5–0.6, followed by a stabilization at a high value around 0.6. The fact that this stabilization takes place on the same time-scale as the damping of the radial oscillations and the increase in temperature of the condensate leads us to speculate that all these phenomena are related through a dissipation mechanism whereby the initial excitations in the longitudinal direction (i.e. reflected in the phase differences between adjacent lattice sites) and in the radial directions lead to a re-thermalization of the system at a higher temperature and hence lower condensate fraction, with the remaining condensate now in the ground state of the combined harmonic and periodic trapping potentials. More detailed theoretical investigations in this direction are planned for the future.

We also note here that the tunneling time between adjacent wells is also comparable to the damping time of the visibility fluctuations for the parameters of our experiment. In order to understand better the importance of the various mechanisms, i.e. damping with a possible coupling between the different modes, and re-phasing due to tunneling, it will be important in future to conduct experiments for a range of different parameter combinations for the trap and the lattice. Also, repeating our experiment in a configuration in which more lattice sites are occupied by the condensate will most likely eliminate the intermediate revivals (which require a large fraction of the sites to be in phase, which is less likely for a large number of sites) and leave only the lower envelope (see Fig. 2) of the visibility evolution. Finally, the role of the finite temperature ( $T \approx 0.7 T_c$ ) at which we start our experiment will have to be investigated more closely.

In summary, we have studied the behaviour of a Bose-Einstein condensate non-adiabatically loaded into a one-dimensional optical lattice. The time-evolution of the collective modes thus excited has been characterized through the visibility of the interference pattern as well as its radial width. Both quantities exhibit large initial variations that are strongly damped on a time-scale comparable to the relaxation time of the condensate temperature.

This work was supported by the MURST (PRIN 2000 Initiative), the INFN (Progetto di Ricerca Avanzata Photonmatter), and by the EU through the Cold Quantum Gases Network, Contract No. HPRN-CT-2000-00125. P.B.B., C.J.W., and P.S.J. acknowledge support from the U.S. Office of Naval Research. O.M. gratefully acknowledges financial support from the EU within the

- [1] M.O. Mewes, M.R. Andrews, N.J. van Druen, D.M. Kum, D.S. Durfee, C.G. Townsend, and W. Ketterle, *Phys. Rev. Lett.* 77, 988 (1996).
- [2] D.S. Jin, M.R. Matthews, J.R. Ensher, C.E. Wieman, and E.A. Cornell, *Phys. Rev. Lett.* 78, 764 (1996).
- [3] F. Chevy, V. Bretin, P. Rosenbusch, K.W. Madison, and J. Dalibard, *Phys. Rev. Lett.* 88, 250402 (2002).
- [4] R. Onofrio, D.S. Durfee, C. Raman, M. Kohl, C.E. Kulewicz, and W. Ketterle, *Phys. Rev. Lett.* 84, 810 (2000).
- [5] O.M. Marago, S.A. Hopkins, J. Arit, E. Hodby, G. Hechenblaikner, and C.J. Foot, *Phys. Rev. Lett.* 84, 2056 (2000).
- [6] Damping of condensate excitations due to condensate merging was recently observed by A.P. Chikkatur et al., *Science* 296, 2193 (2002).
- [7] C. Orzel, A.K. Tuchman, M.L. Fenselau, M. Yasuda, and M.A. Kasevich, *Science* 291, 5512 (2001).
- [8] M. Greiner, O. Mandel, T. Esslinger, T.W. Hansch, and I. Bloch, *Nature (London)* 415, 6867 (2002).
- [9] Y.B. Band and M. Trippenbach, *Phys. Rev. A* 65, 053602 (2002).
- [10] O. Morsch, J.H. Müller, M. Cristiani, D. Ciampini, and E. Arimondo, *Phys. Rev. Lett.* 87, 140402 (2001).
- [11] M. Cristiani, O. Morsch, J.H. Müller, D. Ciampini, and E. Arimondo, *Phys. Rev. A* 65, 063612 (2002).
- [12] All uncertainties reported here are one standard deviation combined systematic and statistical uncertainties.
- [13] M. Kramer, L.P. Pitaevskii, and S. Stringari, *Phys. Rev. Lett.* 88, 180404 (2002).
- [14] J.M. Ziman, *Principles of the Theory of Solids*, Cambridge University Press (1964).
- [15] M. J. Steel and Weiping Zhang, *cond-mat/9810284* (1998).
- [16] F. Dalfovo, S. Giorgini, L.P. Pitaevskii, and S. Stringari, *Rev. Mod. Phys.* 71, 463-512 (1999)
- [17] We note that  $\epsilon$  relates to the renormalized coupling strength  $g$  defined in [13] according to  $g = U(1 + \epsilon)$ .